Available online at www.sciencedirect.com
ScienceDirect
Annals of Nuclear Energy 34 (2007) 527–532
annals of NUCLEAR ENERGY
www.elsevier.com/locate/anucene

Least-squares finite-element S_N method for solving three-dimensional transport equation

Hai-tao Ju [a,*], Hong-chun Wu [a], Dong Yao [b], Chun-yu Xian [b]

[a] School of Energy and Power Engineering, Xi'an Jiaotong University, Xi'an 710049, PR China
[b] Nuclear Power Institute of China, Chengdu 610041, PR China

Received 20 July 2006; received in revised form 4 February 2007; accepted 9 February 2007
Available online 12 April 2007

Abstract

A discrete ordinates finite-element method for solving three-dimensional first-order neutron transport equation is proposed using a least-squares variation. It avoids the singularity in void regions of the method derived from the second-order equation. Different from using the standard Galerkin variation applying to the first-order equation, the least-squares variation results in a symmetric matrix, which can be solved easily and effectively. The approach allows a continuous finite-element. To eliminate the discontinuity of the angular flux on the fixed flux boundary in the spherical harmonics method, the equation is discretized using the discrete ordinates method for angular dependency. A three-dimensional transport simulation code is developed and applied to some benchmark problems with unstructured geometry. The numerical results demonstrate the accuracy and feasibility of the method.

1. Introduction

Many effective methods in recent years have been proposed in solving the multi-group neutron transport equation. For the regular geometry problems the equation is generally discretized using the finite difference method or the nodal method (Wager and Muller, 1984; Badruzzaman, 1985) for spacial dependency. For the unstructured geometry problems it is often discretized using the finite-element method (Ackroyd, 1995), based on either the first-order transport equation, the even-parity second-order equation (Morel and McGhee, 1999; Christopher, 1999) or the second-order SAAF equation (Morel and McGhee, 1999). But the second-order form of transport equation contains the inversion of the cross-section, which introduces singularity in void regions (Varin and Samba, 2005). To eliminate the singularity, the cross-section in the void region is sometimes assumed to be not zero but $10^{-4}\,cm^{-1}$ so that 3D transport programs based on the second-order differential form can be used (Kobayashi et al., 2000).

Follow a rational line, the first-order transport equation can be solved by the standard Galerkin methods or discontinuous finite-element methods well. However standard Galerkin methods result in a nonsymmetrical system of equations which are difficult to be solved. Meanwhile discontinuous finite-element methods (Ackroyd et al., 1995; Barros, 1997; Wareing et al., 2001; Warsa et al., 2002) are required to accurately treat transport in heterogeneous domain (Varin and Samba, 2005). The equation is hard to be solved when the geometry is complex and multi-dimensional.

An alternative least-squares finite-element has been proposed by Manteuffel and Ressel in the single-group spherical-harmonics transport equation in case of the isotropic scattering (Manteuffel and Ressel, 1998; Manteuffel et al., 2000). The equation has not the inversion of the cross-section, so the method based on it can solve the problem with void regions. Meanwhile least-squares technique can result in a symmetric matrix, which can be solved by the effective methods, such as the Cholesky method or conjugate gradient method.

Many studies have been published concerning the spherical harmonics method (P_N) using the least-squares finite-

* Corresponding author.
E-mail address: haitaoju@gmail.com (H.-t. Ju).

0306-4549/$ - see front matter © 2007 Elsevier Ltd. All rights reserved.
doi:10.1016/j.anucene.2007.02.003

element method, but little work has been published on the discrete ordinates method. In realistic problems the spherical harmonics method exhibits discontinuous angular flux on the fixed flux boundary. The flux distribution by the spherical harmonics method shows some anomalies at the material interfaces of large cross-section differences or at the material void interface (Kobayashi et al., 2000). To eliminate the anomaly, the angle variables are better to be discretized by the discrete ordinates method (S_N). Although the discrete ordinates method exhibits ray-effect problems, it is convenient to treat different boundary conditions and requires less CPU time. It is easy to develop a general code for different orders of fully symmetric quadrature set.

Base on above analysis, the least-squares finite-element method was selected to solve the multi-group first-order transport equation in case of anisotropic scattering for the discrete ordinates system. A three-dimensional transport simulation code is developed and applied to the benchmark problems with unstructured geometry.

2. Least-squares finite-element variation of first-order neutron transport equation

2.1. The discrete ordinates discretization of neutron transport equation

The traditional first-order neutron transport equation is

$$\Omega \cdot \nabla \Phi(r,E,\Omega) + \Sigma_t \Phi(r,E,\Omega) = Q_s + Q_f + S \tag{1}$$

where Ω is the unit direction vector and angular variable, r is the space variable, E is the energy variable, $\Phi(r,E,\Omega)$ is the neutron angular flux, Σ_t is the total macroscopic cross-section, Q_s is the scattering source term, Q_f is the fission source term and S is the fixed source term.

First, the energy variable is E discretized by the multi-group approximation. Definition of group angular flux is given as:

$$\Phi_g(r,\Omega) = \int_{\Delta E_g} \Phi(r,E,\Omega)\,dE \quad g = 1,2,\ldots,G \tag{2}$$

Then the Eq. (1) may be written:

$$\Omega \cdot \nabla \Phi_g(r,\Omega) + \Sigma_t \Phi_g(r,\Omega) = Q_{s,g} + Q_{f,g} + S_g \tag{3}$$

The discrete ordinates method is a standard technique to obtain numerical solution of transport equation. In the method, the angular variable Ω is discretized into a finite number of directions Ω_m, $m = 1,2,\ldots,N$, and the angular flux is calculated for each direction. Integrating Eq. (3) over the domain $\Delta\Omega_m$ at the direction Ω_m, we obtain:

$$\int_{\Delta\Omega_m} [\Omega \cdot \nabla \Phi_g(r,\Omega) + \Sigma_t \Phi_g(r,\Omega)]\,d\Omega = \int_{\Delta\Omega_m} [Q_{s,g} + Q_{f,g} + S_g]\,d\Omega \tag{4}$$

Here we define the following:

$$\int_{\Delta\Omega_m} \Phi_g(r,\Omega)\,d\Omega = \omega_m \Phi_{m,g}(r) \tag{5}$$

$$\int_{\Delta\Omega_m} [\Omega \cdot \nabla \Phi_g(r,\Omega)]\,d\Omega = \omega_m [\Omega \cdot \nabla \Phi_g(r,\Omega)]_m \tag{6}$$

$$\int_{\Delta\Omega_m} [Q_{s,g} + Q_{f,g} + S_g]\,d\Omega = \omega_m [Q_{s,g} + Q_{f,g} + S_g]_m = \omega_m [Q_{s,m,g} + Q_{f,m,g} + S_{m,g}] \tag{7}$$

where ω_m is the quadrature weight.

Then in the Cartesian X–Y–Z geometry, the discrete ordinates form of the multi-group three-dimensional transport equation can be expressed as follows:

$$\mu_m \frac{\partial \Phi_{m,g}}{\partial x} + \eta_m \frac{\partial \Phi_{m,g}}{\partial y} + \xi_m \frac{\partial \Phi_{m,g}}{\partial z} + \Sigma_t \Phi_{m,g} = Q_{s,m,g} + Q_{f,m,g} + S_{m,g} \tag{8}$$

where μ_m, η_m, ξ_m is the directional cosine, $\Phi_{m,g} = \Phi_g(x,y,z,\mu_m,\eta_m,\xi_m)$ is the neutron angular flux of the point with the coordinate is (x,y,z) in group g at the direction (μ_m,η_m,ξ_m), $Q_{s,m,g}$ is the scattering source term in group g at the direction (μ_m,η_m,ξ_m), $Q_{f,m,g}$ is the fission source term in group g at the direction (μ_m,η_m,ξ_m) and $S_{m,g}$ is the fixed source term in group g at the direction (μ_m,η_m,ξ_m), which is written as

$$\begin{aligned} Q_{s,m,g} &= Q_{s,g}(x,y,z,\mu_m,\eta_m,\xi_m) \\ &= \frac{1}{2\pi} \sum_{l=0}^{L} \frac{2l+1}{2} \sum_{g'=1}^{G} \Sigma_{g'\to g,l} \\ &\quad \cdot \left[P_l(\mu_m) \sum_{m'=1}^{M} \omega_{m'} P_l(\mu_{m'}) \Phi_{g'}(x,y,z,\mu_{m'},\eta_{m'},\xi_{m'}) \right] \\ &\quad + \frac{1}{\pi} \sum_{l=0}^{L} \frac{2l+1}{2} \sum_{g'=1}^{G} \Sigma_{g'\to g,l} \\ &\quad \cdot \left[\sum_{k=1}^{l} \frac{(l-k)!}{(l+k)!} P_l^k(\mu_m) \sum_{m'=1}^{M} \omega_{m'} \cdot P_l^k(\mu_{m'}) \right. \\ &\quad \left. \times \cos k(\varphi_{m'} - \varphi_m) \Phi_{g'}(x,y,z,\mu_{m'},\eta_{m'},\xi_{m'}) \right] \end{aligned} \tag{9}$$

where $\Sigma_{g'\to g,l}$ is the macroscopic scattering cross-section from group g' to g, $P_l(\mu_m)$ is the Legendre polynomials and $P_l^k(\mu_m)$ is the associated Legendre function, in case of the anisotropic scattering source, and

$$\begin{aligned} Q_{s,m,g} &= Q_{s,g}(x,y,z,\mu_m,\eta_m,\xi_m) \\ &= \frac{1}{4\pi} \sum_{g'=1}^{G} \Sigma_{g'\to g} \sum_{m'=1}^{M} \omega_{m'} \Phi_{g'}(x,y,z,\mu_{m'},\eta_{m'},\xi_{m'}) \end{aligned} \tag{10}$$

in case of the isotropic scattering source.

The $Q_{f,m,g}$ is given in the following way:

$$Q_{f,m,g} = \frac{\chi_g}{4\pi k} \sum_{g'=1}^{G} (\nu\Sigma_f)_{g'} \sum_{m'=1}^{M} \omega_{m'} \Phi_{g'}(x,y,z,\mu_{m'},\eta_{m'},\xi_{m'}) \tag{11}$$

For 3D cartesian geometry, the boundaries are planes perpendicular to the coordinate axis. The following are assumed as boundary conditions:

1. The reflective boundary condition:

$$\Phi_{m,g} = \Phi_g(x,y,z,\mu_m,\eta_m,\xi_m) = \Phi_g(x,y,z,\mu_{m'},\eta_{m'},\xi_{m'}) \quad (x,y,z) \in \Gamma_1 \wedge n(x,y,z)\cdot\Omega < 0 \tag{12}$$

where $(\mu_{m'},\eta_{m'},\xi_{m'})$ is the reflective directional cosine of (μ_m,η_m,ξ_m), $n(x,y,z)$ is the normal direction at the point (x,y,z).

2. The vacuum boundary condition:

$$\Phi_{m,g} = \Phi_g(x,y,z,\mu_m,\eta_m,\xi_m) = 0.0 \quad (x,y,z) \in \Gamma_2 \wedge n(x,y,z)\cdot\Omega < 0 \tag{13}$$

Eqs. (8), (12) and (13) can be written in the form of operator:

$$\begin{cases} L\Phi_{m,g} = F & \text{for } (x,y,z,\Omega) \in R \times S^1 \\ \Phi_{m,g} = \Phi_g(x,y,z,\mu_{m'},\eta_{m'},\xi_{m'}) & \text{for } (x,y,z) \in \Gamma_1 \wedge n(x,y,z)\cdot\Omega < 0 \\ \Phi_{m,g} = 0.0 & \text{for } (x,y,z) \in \Gamma_2 \wedge n(x,y,z)\cdot\Omega < 0 \end{cases} \tag{14}$$

2.2. Least-squares finite-element variation formulation of neutron transport equation

A subspace V is given as:

$$V := \{\Phi^0 \in H^1(r^3)\} \tag{15}$$

where $H^1(r^3)$ is a Hilbert space. The least-squares variational formulation of Eq. (14) is given by Manteuffel and Ressel (1998):

$$\min_{\Phi_{m,g}\in V} \widetilde{F}(\Phi_{m,g}), \quad \text{with } \widetilde{F}(\Phi_{m,g}) := \int [L\Phi_{m,g} - F]^2 \,\mathrm{d}r^3 \tag{16}$$

Then the least-squares finite-element discretization problem could be obtained:

$$\begin{cases} \text{Find } \Phi_{m,g} \in V & \text{s.t.} \\ \tilde{a}(\Phi_{m,g},\Phi^0) = \tilde{b}(\Phi^0) & \forall \Phi^0 \in V \end{cases} \tag{17}$$

$$\text{where } \begin{cases} \tilde{a}(\Phi_{m,g},\Phi^0) := (L\Phi_{m,g}, L\Phi^0) = \int L\Phi_{m,g}\cdot L\Phi^0 \,\mathrm{d}r^3 \\ \tilde{b}(\Phi^0) := \int F\cdot L\Phi^0 \,\mathrm{d}r^3 \end{cases} \tag{18}$$

Then, the least-squares finite-element variation formulation of Eq. (14) could be written as

$$\begin{cases} \int\int \left(\mu_m \frac{\partial\Phi_{m,g}}{\partial x} + \eta_m \frac{\partial\Phi_{m,g}}{\partial y} + \xi_m \frac{\partial\Phi_{m,g}}{\partial z} + \Sigma_t\Phi_{m,g}\right)\left(\mu_m \frac{\partial\Phi^0}{\partial x} + \eta_m \frac{\partial\Phi^0}{\partial y} + \xi_m \frac{\partial\Phi^0}{\partial z} + \Sigma_t\Phi^0\right)\mathrm{d}x\,\mathrm{d}y\,\mathrm{d}z = \\ \quad \int\int (Q_{s,m,g} + Q_{f,m,g} + S_{m,g})\left(\mu_m \frac{\partial\Phi^0}{\partial x} + \eta_m \frac{\partial\Phi^0}{\partial y} + \xi_m \frac{\partial\Phi^0}{\partial z} + \Sigma_t\Phi^0\right)\mathrm{d}x\,\mathrm{d}y\,\mathrm{d}z \\ \Phi_{m,g} = \Phi_g(x,y,z,\mu_{m'},\eta_{m'},\xi_{m'}) \quad \text{for } (x,y,z) \in \Gamma_1 \wedge n(x,y,z)\cdot\Omega < 0 \\ \Phi_{m,g} = 0.0 \quad \text{for } (x,y,z) \in \Gamma_2 \wedge n(x,y,z)\cdot\Omega < 0 \end{cases} \tag{19}$$

3. Numerical results

A three-dimensional multi-group transport code, Least-squares finite-element solution of neutron transport equation (LESFES), was developed according to the method described above, by which the eigenvalue problems and fixed source problems could be solved for several benchmark problems. For the resulting matrix is symmetric, it is convenient to use one-dimensional data storage structure in the code. Fast iterative methods could be used to solve the equation. The triangular prism meshes were used in the following problems, which had 15 nodes each. The number of the Gauss integral points was 12. The convergence criterions of eigenvalues and flux are 1.0E−5 and 1.0E−5.

3.1. Small LWR core benchmark

The first benchmark problem represents a small model of a light water reactor (LWR), which is based on the KUCA Facility. The reactor consists of a fuel region having dimensional of $30\times30\times30$ cm, a void region (in place of control rods) of $5\times10\times50$ cm and a reflector region with $5\times10\times50$ cm. The overall dimensions are $50\times50\times50$ cm. The neutron interactions are modeled in two energy groups representing the fast and thermal groups, respectively (Ziver et al., 2005; Tekeda and Ikeda, 1991). The constants (material cross-sections and fission spectrum) are not presented here. The interested reader could refer to the benchmark problem book to obtain the data. The following two cases are considered

Case 1: The control rod position is empty (void).
Case 2: The control rod is inserted.

The number of the meshes is 566. The side and the height of the triangular prism are 5 cm and 15 cm for $0 < z \leqslant 15$ cm, 5 cm and 10 cm for 15 cm $< z \leqslant 25$ cm respectively. The number of unknowns (nodes) is 2158. The eigenvalues K_{eff} and the control rod worth are showed in Table 1. The number of S_N iterations is 126 for both cases.

Due to the limitation of data memory for personal computer, the S_2 fully symmetric quadrature set is used here. Although the order is lowest, the difference of the eigenvalues K_{eff} is only 0.18% and 0.28%, respectively, compared with the Monte-Carlo method. The difference of control

Table 1
The eigenvalues and the control rod worth of small LWR core benchmark

Codes	K_{eff}		Control rod worth
	Rod-out	Rod-in	
Monte-Carlo	0.9778	0.9624	1.64E−2
MARK-P_N	0.9766	0.9630	1.45E−2
LESFES	0.9761	0.9597	1.75E−2

rod worth is 6.7%, which is less than the difference of MARK-P_N code (11.6%).

3.2. Small FBR core benchmark

The benchmark is based on a model representing a small model of a FBR. The dimensions of the model representing the quarter of the core due to symmetry are $70 \times 70 \times 150$ cm. the model composed of a fuelled region, radial and axial blankets and a control rod region. The case that control rods withdrawn has been studied. The material cross-sections (group constants) were available and modeled in four energy groups for the case (Ziver et al., 2005; Tekeda and Ikeda, 1991).

Here we only calculate one case: the control rod is withdrawn (the control rod position is filled with Na). The number of the meshes is 1680. The side and the height of the triangular prism are 5 cm and 20 cm for $0 < z \leqslant 20$ cm, 5 cm and 55 cm for $20 < z \leqslant 75$ cm respectively. The number of unknowns (nodes) is 5441. The eigenvalues K_{eff} and the region-averaged fluxes are shown in Tables 2 and 3, respectively. The number of S_N iterations is 139.

The S_2 fully symmetric quadrature set is used here also. The difference of the eigenvalues is only 0.22% and the difference of MARK-P_N code is 0.64%. Most of the differences of region-averaged fluxes are within 3.0%, except that in the CRP region of fourth region reaches the maximum 13.8%. This is because the order of the fully symmetric quadrature set is low and the mesh size is a little coarse. But the result of MARK-P_N code is not close to the reference, neither and the difference is 13.3%.

3.3. ISSA anisotropic scattering benchmark

The theoretical model described above can be used to solve the problem with anisotropic scattering. But there is no proper three-dimensional benchmark published with anisotropic scattering. So here the one-dimensional ISSA anisotropic scattering benchmark (Issa et al., 1986) is tested using the three-dimensional code LESFES. The 1D benchmark is simply extended to 3D problem with $y = 1$ cm and $z = 1$ cm. Reflective boundary conditions are used at the boundary planes $y = 0$, $y = 1$ cm, $z = 0$ and $z = 1$ cm.

Table 2
The eigenvalues of small FBR core benchmark

Codes	Monte-Carlo	MARK-P_N	LESFES
K_{eff}	0.9732	0.9794	0.9711

Table 3
The region-averaged fluxes of Small FBR core benchmark

Codes	Groups	Core	Axial blanket	Radial blanket	CRP
Monte-Carlo	1G	4.2814E−5	5.1850E−6	3.3252E−6	2.5344E−5
	2G	2.4081E−4	4.6912E−5	3.0893E−5	1.6658E−4
	3G	1.6411E−4	4.6978E−5	3.2834E−5	1.2648E−4
	4G	6.2247E−6	3.7736E−6	2.0473E−6	6.9840E−6
MARK-P_N	1G	4.2370E−5	5.4492E−6	3.5595E−6	2.5130E−5
	2G	2.3926E−4	5.3696E−5	3.5354E−5	1.6795E−4
	3G	1.6679E−4	5.7551E−5	4.0261E−5	1.3187E−4
	4G	6.2855E−6	5.0063E−6	2.6785E−6	7.9182E−6
LESFES	1G	4.1575E−5	5.3595E−6	3.4131E−6	2.8020E−5
	2G	2.3395E−4	4.5999E−5	3.0375E−5	1.6625E−4
	3G	1.5862E−4	4.5237E−5	3.1723E−5	1.2028E−4
	4G	5.9180E−6	3.5048E−6	1.9999E−6	6.0195E−6

The cross-section constants are given in Table 4 and the eigenvalue are given in Table 5. The number of the meshes is 352. The side and the height of the triangular prism are 0.25 cm and 0.50 cm respectively. The number of unknowns (nodes) is 1429. The number of S_N iterations is 22, 23, 25 and 27 for the order of fully symmetric quadrature set is 2, 4, 6 and 8.

From Table 5 we can see that the result is unacceptant using S_2 fully symmetric quadrature set. This is because the precision of S_2 fully symmetric quadrature set is the lowest used in the case of anisotropic scattering. But the relative difference is only 0.024% using the S_6 fully symmetric quadrature set. And the relative difference of S_8 result decreases to 0.018% compared with the reference result using the S_{16}.

Table 4
The cross-section constants for ISSA anisotropic scattering problem (cm^{-1})

Region	Σ_t	$\nu\Sigma_f$	Σ_s^0	Σ_s^n $n = 1.5$
1	1.1	1.0	0.6	0.1
2	0.95	0.0	0.55	0.15

Table 5
The eigenvalue for ISSA anisotropic scattering problem

S_n	S_2	S_4	S_6	S_8	S_{16}
Reference	–	–	1.6772	–	1.6784
LESFES	2.1531	1.6738	1.6776	1.6781	–
P_n	P_1	P_3	P_5	–	–
FELTRAN	1.6451	1.6751	1.6771	–	–

Table 6
The cross-section for problem with a void region

Group	$\nu\Sigma_f/cm^{-1}$	Σ_{1-1}/cm^{-1}	Σ_{1-2}/cm^{-1}	Σ_t/cm^{-1}	χ
1	6.203E−3	1.78E−1	1.002E−2	1.96647E−1	1.0
	$\nu\Sigma_f/cm^{-1}$	Σ_{2-1}/cm^{-1}	Σ_{2-2}/cm^{-1}	Σ_f/cm^{-1}	
2	1.101E−1	1.089E−3	5.255E−1	5.96159E−1	0.0

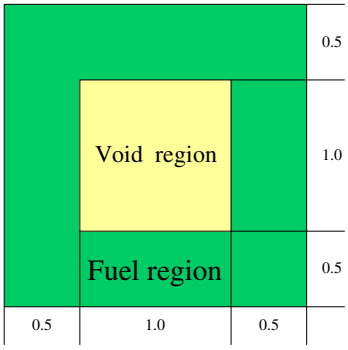

Fig. 1. The x–y plane geometry for problem with a void region.

3.4. Problem with a void region

A problem with a void region was designed. It contains a void region surrounded by fuel. The cross-section and the x–y plane geometry are shown in Table 6 and Fig. 1. Reflective boundary conditions are used at all outer boundaries. The overall dimensions are $2.0 \times 2.0 \times 1.0$ cm. In the calculation, the total cross-section of the void region is set zero. The number of the meshes is 288. The side and the height of the triangular prism are 0.25 cm and 0.50 cm respectively. The number of unknowns (nodes) is 1141. The number of S_N iterations is 59, 62 and 64 for the order of fully symmetric quadrature set is 4, 6 and 8.

The LESFES results are compared with the results of the MG-MCNP3B codes in Table 7. In the MG-MCNP3B calculation, the nominal source size for each cycle is 30000. The number of cycles to skip before beginning tally accumulation is 30. The number of cycles to be done before the problem ends is 100. Compared with the MG-MCNP3B results, the maximum error is about 0.08% for the LESFES flux using the S_4 fully quadrature set and the error decreases when used a higher quadrature set, which is 0.06% for the S_8 set. Meanwhile, for the eigenvalue the difference decreases from 0.06% to 0.04%.

Table 7
Average scalar fluxes for fuel region and eigenvalues for problem with a void region

Code	Group 1	Group 2	K_{eff}
MG-MCNP3B	9.01330	1.27853	1.17988
LESFES (S_4)	9.00748	1.27751	1.17917
LESFES (S_6)	9.00887	1.27766	1.17929
LESFES (S_8)	9.00911	1.27767	1.17935

4. Conclusion

A discrete ordinates finite-element method based on the three-dimensional first-order neutron transport equation is derived using the least-squares variation and also the simulation code is developed. The multi-group neutron transport equation for the unstructured geometry with a severe anisotropic scattering was solved with a good accuracy. Although the S_2 fully symmetric quadrature set were used in the small LWR and FBR benchmark, the results were in agreement with the reference. The ISSA anisotropic scattering problem indicated that the calculated results were quite close to the reference results. The code developed in this paper could also treat problem with void regions. Overall it has been demonstrated that the least-squares finite-element method used in the first-order transport equation could handle the multi-group anisotropic or isotropic scattering problems with unstructured geometry successfully.

Acknowledgements

This work is supported by National Natural Science Foundation of China Grant No. 10475064 and National Key Laboratory of Reactor System Design Technology Grant No. SYX-01-05-09.

References

Ackroyd, R.T., 1995. Foundation of finite element applications to neutron transport. Prog. Nucl. Energ. 29, 43.

Ackroyd, R.T., Abuzid, O.A., Mirza, A.M., 1995. Discontinuous finite element solutions for neutron transport in x–y geometry. Ann. Nucl. Energ. 22, 181.

Badruzzaman, A., 1985. An efficient algorithm for nodal-transport solutions in multidimensional geometry. Nucl. Sci. Eng. 89, 281.

Barros, R.C., 1997. On the equivalence of discontinuous finite element methods and discrete ordinates methods for the angular discretization of the linearized boltzmann equation in slab geometry. Ann. Nucl. Energ. 24, 1013.

Christopher, J.G., 1999. Finite element methods for second order forms of the transport equation. Dissertation of Texas A&M University, USA.

Issa, J.G., Riyait, N.S., Goddard, A.J.H., et al., 1986. Multigroup application of the anisotropic FEM code FELTRAN to one, two, three-dimensional and R–Z problems. Prog. Nucl. Eng. 18 (1), 251.

Kobayashi, K., Sugimural, N., Nagaya, Y., 2000. 3-D radiation transport benchmark problems and results for simple geometries with void regions. NEA-OECD. NOV.

Manteuffel, T.A., Ressel, K.J., 1998. Least-squares finite-element solution of the neutron transport equation in diffusive regimes. Siam. J. Numer. Anal. 35, 806.

Manteuffel, T.A., Ressel, K.J., Starke, G., 2000. A boundary functional for the least-squares finite-element solution of neutron transport problems. Siam. J. Numer. Anal. 37, 556.

Morel, J.E., McGhee, J.M., 1999. A self-adjoin angular flux equation. Nucl. Sci. Eng. 132, 312.

Tekeda, T., Ikeda, H., 1991. 3-D neutron transport benchmarks. J. Nucl. Sci. Technol. 28 (7), 656.

Varin, E., Samba, G., 2005. Spherical harmonics finite element transport equation solution using a least-squares approach. Nucl. Sci. Eng. 151, 167.

Wager, M.R., Muller, B., 1984. The nodal discrete ordinates method and its application to LWR lattice problems. Topical Meeting on Reactor Physics and Shielding. American Nuclear Society, Chicago, USA.

Wareing, T.A., McGhee, J.M., Morel, J.E., Pautz, S.D., 2001. Discontinuous finite element Sn methods on three-dimensional unstructured grids. Nucl. Sci. Eng. 138, 256.

Warsa, J.S., Wareing, T.A., Morel, J.E., 2002. Fully consistent diffusion synthetic acceleration of linear discontinuous Sn transport discretizations on unstructured tetrahedral meshes. Nucl. Sci. Eng. 141, 236.

Ziver, A.K., Shahdatullah, M.S., Eaton, M.D., 2005. Finite element spherical harmonics (Pn) solutions of the three-dimensional Takeda benchmark problems. Ann. Nucl. Energ. 32, 925.